GPS Solutions (2020) 24:82
https://doi.org/10.1007/s10291-020-00994-z

ORIGINAL ARTICLE

Site-specific real-time GPS multipath mitigation based on coordinate time series window matching

Nan Shen[1] · Liang Chen[1,2] · Lei Wang[1,2] · Xiangchen Lu[1] · Tingye Tao[3] · Jun Yan[4] · Ruizhi Chen[1,2]

Received: 29 August 2019 / Accepted: 4 June 2020

Abstract

Multipath effect is one of the main errors in precise global navigation satellite system (GNSS) positioning. Although there are many GNSS multipath mitigation models available, each model has some limitations. We discuss the problem of mitigating low-frequency multipath in a specific site from the coordinate domain. At present, sidereal filtering is one of the most commonly used methods, in which the repetition period of multipath has to be estimated before multipath mitigation. However, in such a method, the maneuver of the satellite orbit and the long ephemeris update interval will cause inaccurate estimation of the repetition period. We propose a variation of the sidereal filtering method based on window matching. In that method, the window of coordinate time series formed by the current epoch and several previous epochs is used as the query window, and the matched window is searched in the time series of the previous day. The degree of similarity between windows is evaluated by similarity measures. Based on the coordinate point pairs in the matching window, multipath mitigation of the current epoch is performed by an affine transformation. The effects of different similarity measures in window matching are explored, and an early and late matching algorithm is proposed to solve the ambiguous problem of multiple matching sequences in integer-valued similarity metrics. Two sets of short baseline data were collected by different types of receivers in harsh environments to validate the method. The results show the feasibility and effectiveness of the proposed method for site-specific real-time multipath mitigation.

Keywords Sidereal filtering · Multipath mitigation · GPS · Window matching · Similarity metric

Introduction

GNSS positioning accuracy is affected by many error sources, of which multipath error is one that is difficult to handle. The GNSS antenna receives signals not only from direct paths but also from indirect paths caused by signal reflection or diffraction from surrounding objects, resulting in differences in phase and amplitude of signals. This phenomenon is called the multipath effect. Multipath effects can seriously degrade GNSS positioning accuracy and is one of the main error sources in GNSS positioning. Although there are models to deal with GNSS multipath problems, having many limitations (Hofmann-Wellenhof et al. 2012; Jin et al. 2014; Wang et al. 2018), it is thus still an open problem to

✉ Liang Chen
l.chen@whu.edu.cn

Nan Shen
nanshen@whu.edu.cn

Lei Wang
lei.wang@whu.edu.cn

Xiangchen Lu
2018286190164@whu.edu.cn

Tingye Tao
taotingye@hfut.edu.cn

Jun Yan
yanj@njupt.edu.cn

Ruizhi Chen
ruizhi.chen@whu.edu.cn

[1] State Key Laboratory of Information Engineering in Surveying, Mapping and Remote Sensing, Wuhan University, Wuhan 430079, China

[2] Collaborative Innovation Center for Geospatial Technology, Wuhan 430079, Hubei, China

[3] Hefei University of Technology, Hefei 230009, Anhui, China

[4] College of Telecommunications and Information Engineering, Nanjing University of Posts and Telecommunications, Nanjing 210003, China

Published online: 19 June 2020

effectively eliminate the multipath effect on precise GNSS positioning.

In the past decades, methods have been explored to eliminate or reduce multipath effects. For high precision GNSS applications, the most popular way to handle the multipath effect is by choosing a benign environment for GNSS signal tracking. But this method depends on circumstances since it might not be easy to find a site completely free of multipath effects. In addition, it is not feasible to choose a benign environment for dynamic applications (Misra and Enge 2006; Ye et al. 2015). Hardware-based multipath elimination strategy is an effective solution, but the cost is high (Jia et al. 2018; Townsend et al. 1995).

There is also a widely studied multipath processing strategy: data processing algorithms. Multipath mitigation algorithms are mainly divided into two categories: multipath detection algorithms and direct multipath mitigation algorithms. Threshold detection is the most commonly used method in multipath detection, and signal-to-noise ratio (SNR) is often used as a detection index (Groves et al. 2013; Strode and Groves 2016; Zhang et al. 2019). However, the determination of the threshold needs to be acquired in a non-multipath environment, and whether the threshold is related to hardware needs further study (Strode and Groves 2016). In recent years, some machine learning algorithms have been introduced for multipath detection (Chen et al. 2012, 2014; Hsu 2017; Quan et al. 2018). However, the down-weight or removal strategy after detection needs further study (Lau and Cross 2006).

There are many direct multipath processing strategies available. A multipath model based on ray-tracing has been proposed. The precondition of applying this method is to know in detail the relative permittivity of the reflective surface, the correlator spacing of the receiver, the right-hand circularly polarized (RCP) gain mode of receiving antenna, and the phase center offset and change table (Lau and Cross 2007). The multipath problem is quite complex, and it is difficult to give a unified mathematical model to solve the multipath problem in various applications. However, some application-specific solutions can be given for specific applications. Taking GNSS-based structural health monitoring as an example, the environment around a monitoring site is stable, and the multipath caused by the surrounding environment will appear in the following day (Shen et al. 2019). Another application with similar multipath characteristics is GPS seismology. With the development of Smart Earth and Smart City, there is an increasing demand for such applications (Li and Shao 2009; Li et al. 2010; Shao and Li 2011). Multipath mitigation techniques in such applications are referred to as site-specific multipath mitigation techniques.

As a site-specific multipath mitigation tool, sidereal filtering (SF) was first applied to GPS seismology (Genrich and Bock 1992), the data from the previous sidereal day (23 h 56 m 4 s) were used as a correction for current observation. It was found that the repetition periods of satellite orbits vary, which are significantly different from the nominal values of a sidereal day (Axelrad et al. 2005; Choi et al. 2004). In addition to the orbit repeat time method (ORTM), the aspect repeat time adjustment (ARTA) and the cross-correlation method (CCM) have been studied to estimate the multipath repetition period (MRP) (Agnew and Larson 2007; Larson et al. 2007; Wang et al. 2018). Some studies have compared the filtering effects of observation and coordinate value domains, and different conclusions have been drawn (Lau 2012; Ragheb et al. 2007). The effectiveness of the observation domain sidereal filtering for GPS precise point positioning is evaluated, in which the multipath repetition period is calculated by ORTM and ARTA, respectively, and it is concluded that the observation domain is more stable than the coordinate domain sidereal filtering (Atkins and Ziebart 2016). The application of sidereal filtering in other GNSS is similar, except that the repetition period of the orbit is different (Ye et al. 2015). A summary of the relevant studies on SF is provided in Table 1. The information of content, estimation method of multipath repetition period, and literature are presented.

Table 1 Site-specific multipath mitigation research based on sidereal filtering

Content	Estimation of MRP	Literature
Propose the repeatability of multipath	A sidereal day (23 h 56 m 4 s)	Genrich and Bock (1992)
Modified SF	ORTM	Choi et al. (2004)
Comparing three MRP estimation methods	ORTM, ARTA	Axelrad et al. (2005)
	ORTM, ARTA, CCM	Wang et al. (2018)
Estimation of GPS MRP	ORTM, ARTA	Agnew and Larson (2007)
Precision improvement of high-rate GPS by SF	ARTA, CCM	Larson et al. (2007)
Comparison of coordinate and observation domain SF	CCM	Ragheb et al. (2007)
	ORTM	Lau (2012)
Effectiveness of observation domain sidereal filtering	ORTM, ARTA	Atkins and Ziebart (2016)
SF of BeiDou	ORTM	Ye et al. (2015)

Accurate estimation of the multipath repetition period is the key to sidereal filtering. Due to the effects of satellite maneuver adjustments, the repeat period of the satellite orbit varies. Due to the existence of the satellite ephemeris update interval, the accurate real-time estimation of the multipath repetition period is limited to a certain extent. Moreover, in the coordinate domain sidereal day filtering method, the problem of satellite switching must be considered, i.e., adjusting the multipath repetition period dynamically according to whether a satellite becomes available or unavailable in each epoch, which makes the implementation more complicated.

Although there are several methods to estimate the multipath repetition period, it is difficult to obtain a consistent estimate from the various methods (Atkins and Ziebart 2016; Wang et al. 2018; Agnew and Larson 2007). From the definition of ORTM (Larson et al. 2007), it can be seen that ORTM estimates the multipath repetition period through the orbital repetition period, without considering the relevant information of the station at all. ARTA estimates the multipath repetition period based on the repetition of the line of sight vector from the station to the satellite, taking into account the relevant information of the station (Axelrad et al. 2005; Wang et al. 2018). Although CCM is a data-driven multipath repetition period estimation method, it is noticed that CCM is based on the mean value of a window to obtain a multipath repetition period, real-time multipath mitigation is carried out epoch by epoch. In addition, there are short-term variations in the multipath repetition period estimation because when the window size in the CCM is set to a different value, the estimated multipath repetition period is different (Ragheb et al. 2007).

The purpose of this research is to find a straightforward and feasible real-time multipath filtering scheme to avoid the complex estimation process of the multipath repetition period. We try to match the coordinate time series window formed by the current epoch and the previous epochs with the coordinate time series of the previous day. Different similarity measures are used for window matching, and the nominal sidereal day is used to narrow down the search range of the previous day. According to the time series in the matched window, the least-squares method is used to determine the approximately linear relationship of the 2-day time series near the current epoch for multipath mitigation.

Therefore, we propose a sidereal filtering scheme based on window matching. A variation of sidereal filtering based on the window matching model is proposed first. The experiments and results are presented next, followed by a discussion of the main issues of the proposed method, and the conclusions.

Methods

Before introducing window matching based coordinate domain sidereal filtering, the similarity and variation of the coordinate time series of two consecutive days are presented and the window matching of coordinate time series between two consecutive days is defined. At present, the scope of this study is limited to the elimination of low-frequency multipath components in the coordinate domain, and the application of this method in the observation domain will be carried out in the follow-up study.

Similarity and variation of the coordinate time series between two consecutive days

For the coordinate time series obtained by the traditional positioning model, there is the following relationship:

$$x(t) = \tilde{x}(t) + d(t) + v \tag{1}$$

where $x(t)$ is coordinate time series of the single epoch solution at t, $\tilde{x}(t)$ is the true value of the coordinates at t, $d(t)$ is the unmodeled errors that are not taken into account in the positioning model, such as the multipath effect, and v is the random noise satisfying the Gaussian distribution $v \sim N\left(0, \sigma^2\right)$. The time series of two consecutive days can be expressed as:

$$\left.\begin{aligned} x\left(t_1(i)\right) &= \tilde{x}\left(t_1(i)\right) + d\left(t_1(i)\right) + v \\ x\left(t_2(j)\right) &= \tilde{x}\left(t_2(j)\right) + d\left(t_2(j)\right) + v \end{aligned}\right\} \tag{2}$$

where $x\left(t_1(i)\right)$ denotes the coordinate of the i th epoch at $t_1(i)$ on the first day, and $x\left(t_2(j)\right)$ represents the coordinate of the j th epoch at $t_2(j)$ on the second day. For the coordinate time series window of a specific site, if errors other than multipath are accurately modeled in the positioning model, the time series for two consecutive days are similar due to the multipath repetition characteristic, as shown in Fig. 1.

These coordinate time series are the relative positioning results of GPS L_1 and L_2 observation data, and the experiment and processing strategies will the sections below. The similarities of the east, north and up components of coordinate time series over two consecutive days are given in the top, middle and bottom panels, respectively. Each panel demonstrates about an hour of the coordinate component time series with coarse alignment, which was collected in two consecutive days. The offset of the time series of the first day and the time series of the second day is manually set to 236 s according to the nominal sidereal day (23 h 56 m 4 s) (Axelrad et al. 2005; Choi et al. 2004). The enlarged view of the highlighted red rectangular in each panel is responsible for displaying the similarity of coordinate time series in detail. These time series reveal the low-frequency similarity in the long-term time series. However, due to random noise,

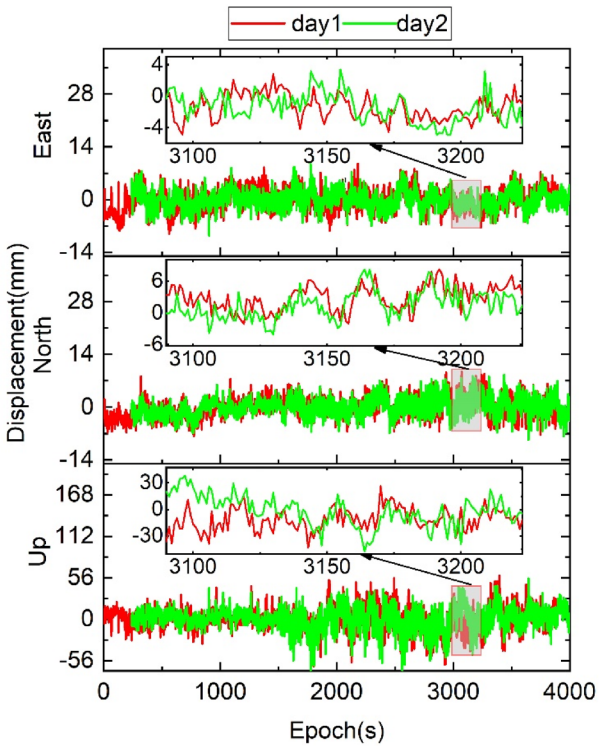

Fig. 1 Similarity of consecutive 2-day coordinate time series with coarse alignment

not all coordinate time series are perfectly matched. In addition, the total error magnitude of the first-day coordinate time series is larger than that of the second day. Although the up component varies much larger than the other two components, similarity still exists in the coordinate time series for two consecutive days. Based on the similarity of the coordinate time series window, the complicated process of the accurate estimation of the multipath repetition period can be omitted. The relevant definitions of coordinate time series window matching for two consecutive days are given below.

Window matching of coordinate time series between two consecutive days

For the i th epoch of the second day at $t_2(i)$, the coordinates of $l-1$ epochs before the epoch are taken to form the following coordinate time series template window, also known as query window:

$$x(t_2(i-l+1)),\ x(t_2(i-l+2)),\ldots,x(t_2(i-1)),\ x(t_2(i)) \quad (3)$$

where l is the length of the template window, and i is the index of any epoch in the second day at $t_2(i)$. The approximate time of the matching window on the first day with the template window can be obtained from the approximate multipath repetition period, i.e., the nominal sidereal day T_{sidereal} (23 h 56 m 4 s) (Axelrad et al. 2005; Choi et al. 2004):

$$t_{\text{coarse}} = t_2(i) - T_{\text{sidereal}} \quad (4)$$

This approximate time t_{coarse} is called coarse alignment time on the first day. After obtaining the coarse alignment time, the matching with the defined template window is carried out forward and backward along the coarse alignment time. As shown in Fig. 2, the search is performed in the search window. The similarity between windows is measured by similarity measures, and a brief introduction of the similarity measures will be given below.

Similarity measure of coordinate time series

To determine the similarity of coordinate time series windows, the similarity measure of time series is the key. There are various time series similarity measures. Some scholars have used public data sets for empirical evaluation of different similarity measures, but there is no similarity measure suitable for any data set (Wang et al. 2013, Serrà and Arcos 2014). Six commonly used similarity measures are adopted here, of which three are the lock-step measures, and the other three are elastic measures. The lock-step similarity measure has the advantage of being intuitive and low computational complexity. However, this type of measure is sensitive to

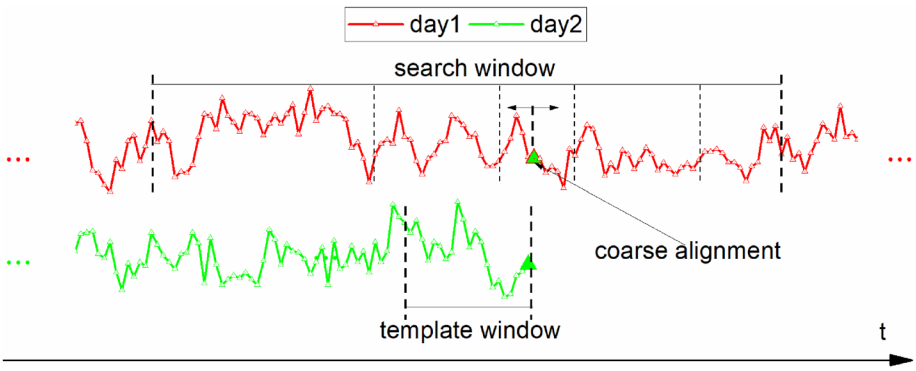

Fig. 2 Window matching of coordinate time series between two consecutive days

noise and time misalignment due to comparing data points one-to-one (Wang et al. 2013). Three lock-step similarity measures are used here: Euclidean distance (ED) (Serrà and Arcos 2014), correlation-based distance (CBD) (Golay et al. 1998), and Fourier coefficient-based distance (FCBD) (Serrà and Arcos 2014). The elastic measure does not require the one-to-one data comparison, that is, one to many comparisons are allowed, which is not sensitive to noise and time misalignment (Wang et al. 2013). However, the elastic similarity measure is usually not intuitive but complicated. Three elastic measures are adopted: dynamic time warping (DTW) (Giorgino 2009), longest common subsequence (LCSS) (Kollios et al. 2002), and edit distance on real sequences (EDR) (Chen et al. 2005). The comparison between lock-step measure and elastic measure is demonstrated as Fig. 3.

The similarity measures have different characteristics. ED, CBD, and FCBD are real-valued metrics, so in most cases, there will not be multiple matching sequences with the same metric value. The other three are integer-valued metrics, so there are problems with multiple matching sequences. The problem of multiple matching in elastic measures can be improved by adding or reducing matching elements in the template window. The improvement scheme is realized by narrowing and expanding the template window. The pseudocode of this algorithm is presented in Table 2.

Multipath mitigation based on affine transformation

The window matching of coordinate time series has been presented in the previous paragraphs. The multipath mitigation solution after window matching is given here. According to the previous analysis, the details of the coordinate time series for two consecutive days have similarities, which are mainly determined by the repeating characteristics of the multipath. For coordinate time series window that has already been matched, the following model is given:

Table 2 Ambiguity free early–late matching algorithm

Pseudocode 1 Ambiguity free early–late matching algorithm

Input: template window, search window

Output: matched window

```
for each window in the search window do
    execute basic window matching
end for
if only one matched window then
    return matched window
end if
repeat
    narrowing template window size
    do standard window matching
    if only one matched window then
        return matched window
    end if
until reaching the minimum window size
repeat
    expanding template window size
    do standard window matching
    if only one matched window then
        return matched window
    end if
until reaching the maximum window size
```

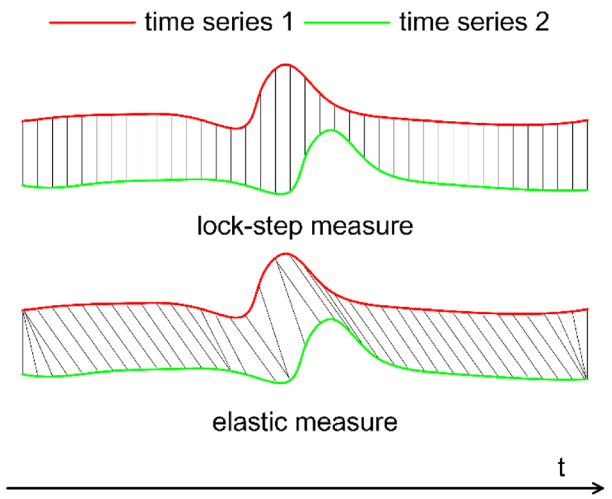

Fig. 3 Comparison of lock-step measure and elastic measure

$$\mathbf{y} = \begin{bmatrix} x_2(1) \\ x_2(2) \\ \vdots \\ x_2(N) \end{bmatrix} = \begin{bmatrix} x_1(1) & 1 \\ x_1(2) & 1 \\ \vdots & \vdots \\ x_1(N) & 1 \end{bmatrix} \begin{bmatrix} a \\ b \end{bmatrix} + \boldsymbol{\varepsilon} = \mathbf{A}\boldsymbol{\alpha} + \boldsymbol{\varepsilon} \tag{5}$$

$$\mathbf{A} = \begin{bmatrix} x_1(1) & 1 \\ x_1(2) & 1 \\ \vdots & \vdots \\ x_1(N) & 1 \end{bmatrix}$$

$$\boldsymbol{\alpha} = \begin{bmatrix} a \\ b \end{bmatrix}$$

where a is the scaling factor, b is the translation factor, and $\boldsymbol{\varepsilon}$ is random noise, and N is the size of the window. The parameters a and b can be estimated by using the time series in the matched window. The minimum sum of squares of residuals is the criteria to determine parameters. Residual is defined as:

$$\mathbf{V} = \mathbf{y} - \mathbf{A}\boldsymbol{\alpha} \tag{6}$$

According to the above conditions, the optimal estimation of parameters should satisfy the following conditions:

$$\hat{\boldsymbol{\alpha}} = [\hat{a}, \hat{b}] = \arg\min_{\alpha} \mathbf{V}^T\mathbf{P}\mathbf{V} \tag{7}$$

where $\mathbf{P}$ is the weight matrix of the coordinate points in the matched window, and the closer to the current epoch, the greater the weight. The parameters can be estimated based on the least square method as follows:

$$\hat{\boldsymbol{\alpha}} = [\hat{a}, \hat{b}] = (\mathbf{A}^T\mathbf{P}\mathbf{A})^{-1}\mathbf{A}^T\mathbf{P}\mathbf{y} \tag{8}$$

Assuming that the matched window and the corresponding parameters have been accurately determined, the estimate $\hat{x}(i+1)$ of next epoch is:

$$\hat{x}_2(i+1) = x_2(i+1) - \hat{a} * x_1(i+1) - \hat{b}, \quad i \in (1 \ldots N) \tag{9}$$

Considering only the low-frequency component of the multipath and the limited time range of the window, we can assume that the multipath can be eliminated by (9). According to covariance propagation law, the variance of the estimate $\hat{x}_2(i+1)$ is calculated as follows:

$$\rho^2_{\hat{x}_2} = \hat{a}^2\rho^2_{x_1} + \rho^2_{x_2} \tag{10}$$

where $\rho^2_{x_1}$ and $\rho^2_{x_2}$ are the variances of coordinate time series of two consecutive days, respectively. From the above deduction, it can be concluded that the noise of the coordinate time series of the previous day is propagated into the final estimation.

Denoising the coordinate time series of the previous day

Besides multipath effects, another main error in coordinate time series is random noise. As mentioned above, if the coordinate time series of the previous day is used for the multipath mitigation of the following day without denoising, the effect of noise will be propagated while performing multipath mitigation.

As an effective component extraction and denoising tool, wavelets are widely used in the fields of images, audio, and other fields. Wavelet analysis technology is adopted to denoise the coordinate time series of the previous day. The discrete wavelet transform (DWT) is defined as (Mallat 2008):

$$\mathrm{DWT}(m,n) = \frac{1}{\sqrt{a_0^m}} \sum_k x[k]\psi\left[a_0^{-m}n - k\right] \tag{11}$$

where $x[k]$ is a discrete signal, $\psi[\sim]$ is the mother wavelet, the integer m is the scaling parameter, the integer n is the time-shift parameter, and a_0 is the scaling step. Wavelet

Table 3 Coordinate time series denoising based on wavelet thresholding

Procedure 1 coordinate time series denoising steps

Input: coordinate time series

Output: denoised coordinate time series

Step 1 Decompose the coordinate time series by discrete wavelet transform (DWT) and get wavelet transform coefficients: C_l, where l is the index of the coefficient, and the number of coefficients is determined by the mother wavelet.

Step 2 The wavelet transform coefficients C_l are quantized by a threshold function. There are two commonly used wavelet thresholds: hard thresholding and soft thresholding.

Hard thresholding:

$$C_l = \begin{cases} C_l, if\,|C_l| > \lambda \\ 0, otherwise \end{cases}$$

or

Soft thresholding:

$$C_l = \begin{cases} sign(C_l)(|C_l| - \lambda), if\,|C_l| > \lambda \\ 0, otherwise \end{cases}$$

Step 3 Perform inverse discrete wavelet transform (IDWT) by using the modified coefficients.

return denoised coordinate time series

thresholding is used to denoise the coordinate time series of the previous day, and the steps are shown in Table 3.

Procedure of sidereal filtering based on window matching

In the previous paragraphs, the similarity of the coordinate time series for two consecutive days is presented, and the definition of window matching of coordinate time series is given. The multipath mitigation strategy after matching and the denoising scheme of the previous day's coordinate time series are given, respectively. The flowchart of sidereal filtering based on window matching is given in Fig. 4.

As shown in Fig. 4, prior to performing the window matching, the template window and the search window must be formed. The template window is formed according to (3), and the search window is constructed according to (4). After determining the template window and the search window, the window matching is carried out based on the similarity measure. Upon completion of the window matching, the process of parameter estimation is carried out according to (8) based on the matched window pair. Then, based on the estimated parameters and the denoised matching coordinate, the current epoch multipath is estimated by the affine transformation. Finally, the estimated multipath is subtracted from the current unfiltered coordinate to obtain the filtered coordinate.

Experiments and results

To verify the feasibility and effectiveness of the proposed method in multipath mitigation, we have carried out experiments in complex environments. The baselines in these experiments are short baselines, and most of the errors except multipath can be canceled out by the relative positioning model. In addition, the method is validated by different receivers. The results before and after multipath mitigation are given in the form of time series graphs and spectrograms, respectively.

Field experiments

Experiments were carried out on the roof of a building in Wuhan University campus. In the experiments, the equipment deployment and surrounding environment are shown in Figs. 5 and 6. In Fig. 5, two geodetic receivers manufactured by CHCNAV were used, one of which serves as a reference station and the other as a rover station. This baseline is about 8 m long and most atmospheric-related errors can be eliminated. As demonstrated in the figure, the environment around the experiment site is complex, and the observation data are susceptible to multipath effects. The experiment lasted 2 days, from March 31, 2019, to April 1, 2019. In Fig. 6, this experiment was conducted at the same location as the previous experiment, but the low-cost receiver uBlox (EVK-M8U) was adopted as a rover. This baseline is about 10 m long and most atmospheric-related errors can

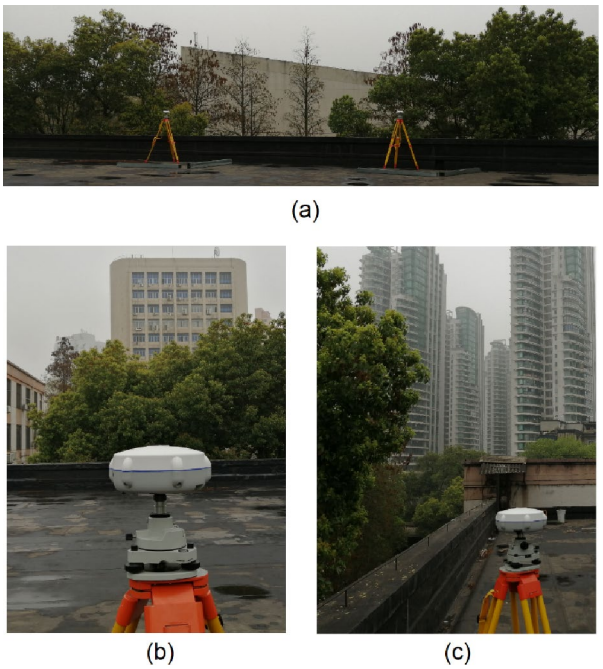

Fig. 5 Baseline between two geodetic receivers. **a** Baseline between two geodetic receivers, **b** rover station: a geodetic receiver; **c** base station: a geodetic receiver

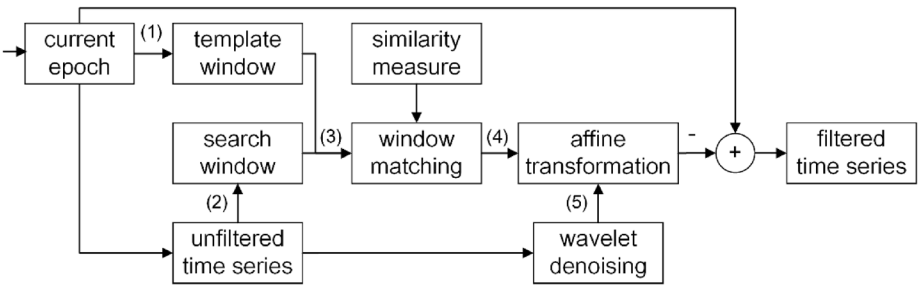

Fig. 4 Sidereal filtering based on window matching

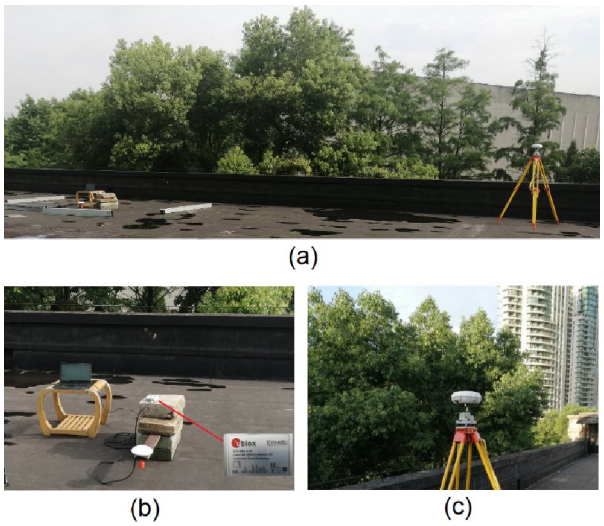

Fig. 6 Baseline between a geodetic receiver and a low-cost receiver. **a** Baseline a geodetic receiver and a low-cost receiver; **b** rover station: a low-cost receiver; **c** base station: a geodetic receiver

be eliminated. Since uBlox does not have data storage capabilities, a laptop is deployed for real-time data collection. The experiment lasted 2 days, from June 30, 2019, to July 1, 2019.

The same processing strategy was used to process the data collected by the above two experiments. First, the observation data are processed by the open-source software RTKLIB (Takasu 2011), using the single epoch kinematic mode. Then the obtained coordinate time series is adopted as the input of the multipath mitigation method.

Case 1: baseline between two geodetic receivers

The first- and second-day observations of the baseline are processed by a single epoch dynamic processing mode, respectively. Then, the time series of the following day is processed epoch by epoch according to the previously proposed window matching based sidereal filtering with the ED as the similarity measure. The results are shown in Fig. 7. The root mean square (RMS) of the coordinate time series is at the top of each panel.

As shown in Fig. 7, after processed by the proposed window matching based sidereal filtering with the ED as the similarity metric, the RMS of east component is reduced from 2.366 to 1.713 mm, and the RMS of north component is reduced from 2.454 to 1.616 mm. Although the RMS of the horizontal component of the first-day coordinate time series is larger than that of the second-day coordinate time series, the accuracy of the second-day coordinate time series can be effectively improved by using the proposed method. The RMS of the east component and the north component

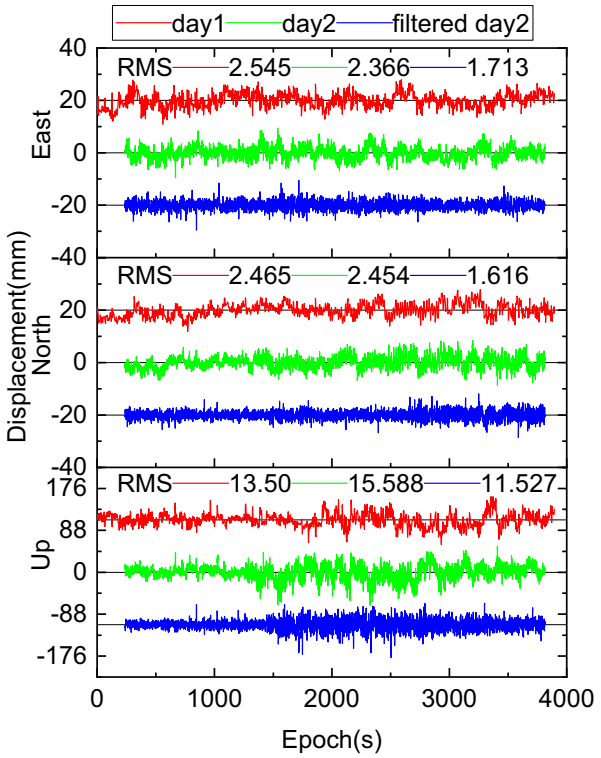

Fig. 7 Processing results in case 1 with the ED as the similarity metric. Red (first-day time series), green (second-day time series), blue (filtered time series of the second day). The time series of the first day and the filtered time series of the second day have been offset from the time series of the second day for clarity. The top, middle, and bottom panels represent the east, north, and up coordinate components, respectively

of the coordinate time series are reduced by 27.61% and 34.16%, respectively. The RMS of the vertical component of the second-day coordinate time series is reduced from 15.588 mm to 11.527 mm. Due to the influence of vertical noise, the RMS of up component of the coordinate time series is reduced by only 26.05%.

For another similarity measure that may have multiple matches: EDR, similar filtering results are shown in Fig. 8. Because the processing mode simulates the real-time single epoch processing mode, the observation noise is not processed. The results showed that there is obvious noise, but it could be seen that the similar components of time series in two consecutive days are significantly eliminated. Because of the limited space, the time series obtained by other similarity measures are not presented here.

To further study the effect of the proposed algorithm on multipath mitigation, we use the fast Fourier transform (FFT) to analyze the time series before and after processing. The results of Fourier transform analysis of coordinate time series are shown in Fig. 9. From comparing the frequency components before and after being processed, it can be seen that the frequency components below 0.01 are

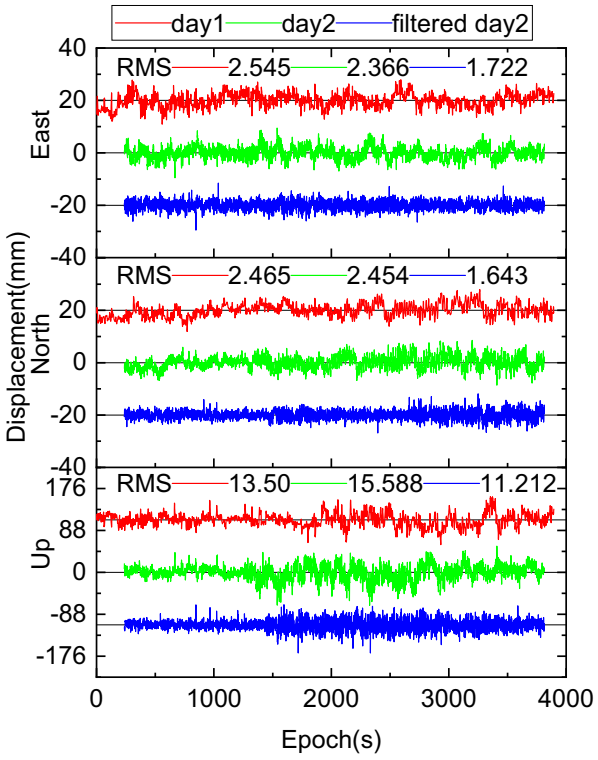

Fig. 8 Processing results in case 1 with EDR as the similarity metric

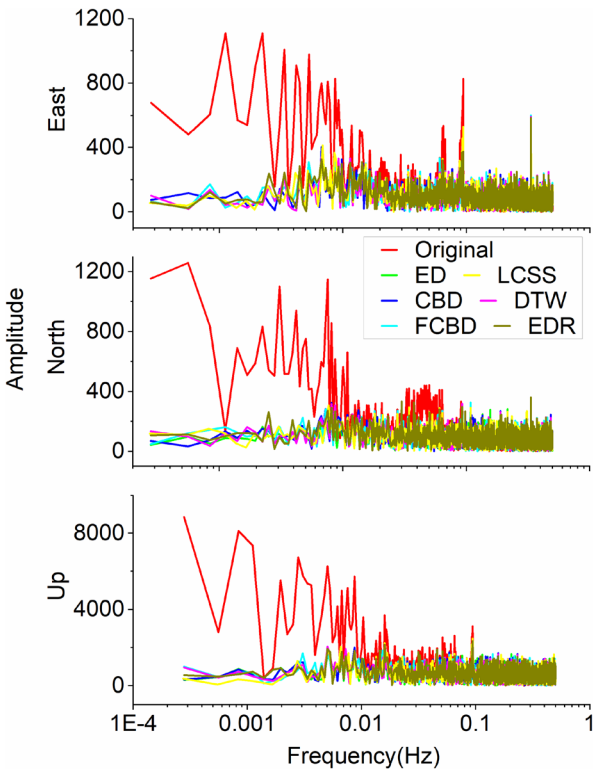

Fig. 9 Frequency components of coordinate time series in case 1 before and after being processed by the proposed method with different similarity measures. Red represents the frequency components of the original coordinate time series and the other colors are the frequency components of the processed coordinate time series using different similarity metrics

significantly mitigated. Previous studies have shown that the multipath components of carrier phase observations lie in the frequency band between 1/2400 and 1/120 Hz (Han and Rizos 1997). As can be seen from the above analysis, multipath components are effectively mitigated by the proposed method with different similarity metrics. In addition, although the low-frequency components of the three coordinate components are different, they are eventually mitigated effectively.

The RMS of the coordinate time series before and after being processed by the proposed method with different similarity metrics is summarized in Table 4. The improvement of the ED metric in the north component is slightly better than other metrics. The improvement of the LCSS measure in the east component is slightly better than other measures. In the up component, the improvement of the EDR measure is better than other measures. In general, the effect of elastic metrics is slightly better than the lock-step measures. In the next section, data from another case are processed and analyzed to evaluate the effectiveness of the method further.

Case 2: baseline between a geodetic receiver and a low-cost receiver

The data processing strategy here is consistent with that in the previous experiment, except that the data come from the low-cost receiver and a geodetic GNSS receiver. The processed time series results with FCBD and LCSS as metrics are shown in Figs. 10 and 11, and the frequency domain analysis results are shown in Fig. 12.

Taking the processing results of the LCSS metric as an example, as demonstrated in Fig. 11, the RMS of the east component is reduced from 2.578 to 1.173 mm, and the RMS of the north component is reduced from 3.445 to 1.50 mm. The RMS of the up component of the second-day coordinate time series is reduced from 12.535 to 5.662 mm. The RMS of the three components of the coordinate time series is reduced by 54.13%, 55.14%, and 54.97%, respectively. The results of frequency analysis are similar to those of the previous experiment.

The RMS of the coordinate time series of this baseline before and after being processed by the proposed method using different similarity metrics is summarized in Table 5. Compared with the statistical values in Table 4, it can be seen that the multipath mitigation effect in this experiment is better than the previous experiment. The possible reason is that in this experiment, there are many objects around the antenna, and it is close to the ground,

Table 4 RMS of coordinate time series in case 1 before and after processing by the proposed method based on different similarity metrics

	East		North		Up	
	RMS (mm)	Improvement (%)	RMS (mm)	Improvement (%)	RMS (mm)	Improvement (%)
Original	2.3657		2.4539		15.5879	
ED	1.7125	27.61	**1.6157**	34.16	11.5273	26.05
CBD	1.7242	27.12	1.6186	34.04	11.5739	25.75
FCBD	1.7285	26.93	1.6492	32.79	11.4346	26.64
DTW	1.7551	25.81	1.6249	33.78	11.4289	26.68
LCSS	**1.7151**	27.50	1.6290	33.62	11.2259	27.98
EDR	1.7221	27.21	1.6433	33.03	**11.2116**	28.07

Bold symbols represent the best measure in the experiment

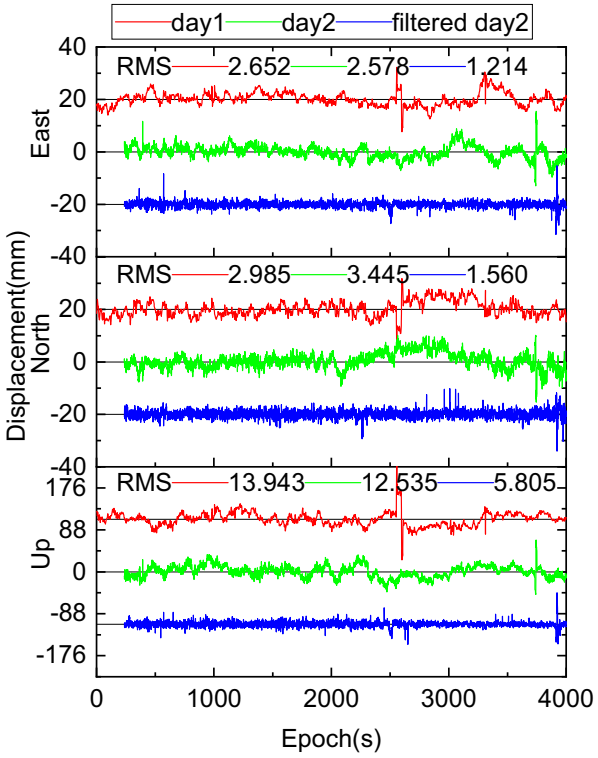

Fig. 10 Processing results in case 2 with FCBD as the similarity metric

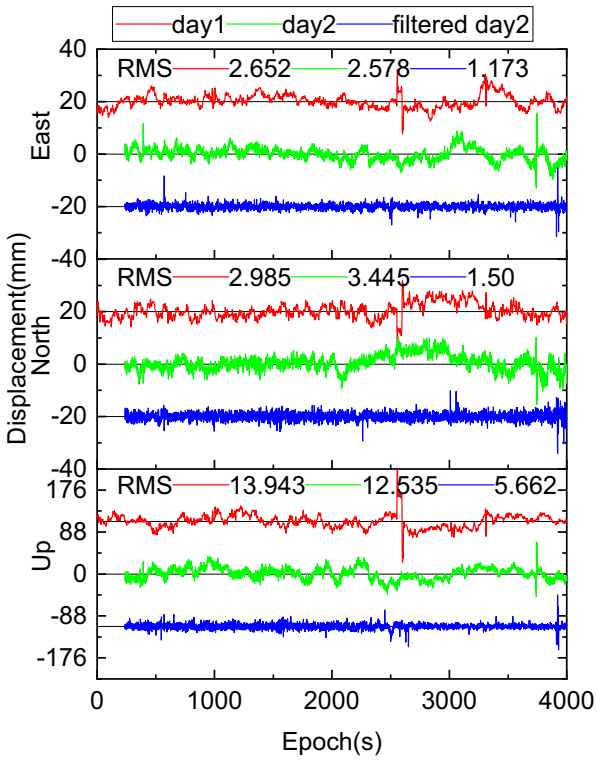

Fig. 11 Processing results in case 2 with LCSS as the similarity metric

which is more susceptible to low-frequency multipath effects (Cai et al. 2016; Fuhrmann et al. 2015; Moore et al. 2014; Ogaja and Satirapod 2007). Another possible reason: compared to geodetic receivers, this type of low-cost navigation receiver does not have multipath suppression strategies at the hardware level or baseband processing level. The coordinate time series resolved from both cases are significantly improved by the proposed method. In contrast to the previous results, the elastic metric results are significantly better than the lock-step metric results.

The feasibility and effectiveness of the proposed method in multipath mitigation have been demonstrated in both time and frequency domains. The factors affecting the effectiveness of the proposed real-time multipath mitigation method will be discussed in the next section.

Discussion

The size of the template window in the window matching based sidereal filtering in the experiments of the previous section is set to 34. The discussion of the effect of

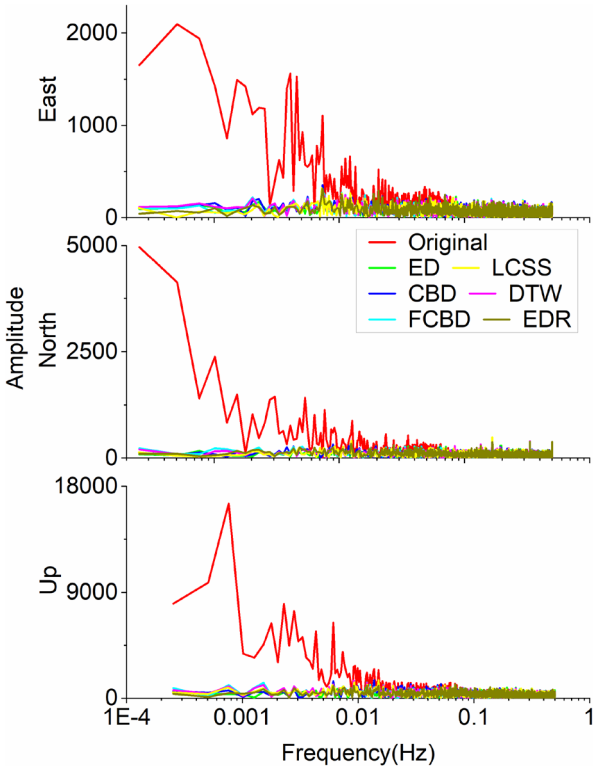

Fig. 12 Frequency components of coordinate time series in case 2 before and after being processed by the proposed method with different similarity measures

template window size on the multipath mitigation effect is given here. In addition, the RMS corresponding to different metrics is given when the template window size takes different values.

Set the appropriate template window size

To further investigate the relationship between the template window size and the accuracy of the sidereal filtering results, we set the size of the template window between 10 and 100, and then get the RMS of the sidereal filtering result. Statistics of different similarity measures are carried out separately. The final statistical results of the two experimental cases are shown in Fig. 13.

As can be seen from Fig. 13, with the increase in template window size, the RMS of the coordinate time series decreases first and then increases. This means that large template window sizes do not necessarily achieve good matching results. The optimum template window size for case 1 is between 20 and 40, while the optimum template window size for case 2 is around 30. Although the optimal value may vary with the receiver and observation environment, the overall trend is consistent and can be obtained by similar statistical methods.

Comparison of similarity measures

In the previous section, the RMS of the sidereal filtering results for different similarity measures is given when the template window size is set to 34. Figure 13 shows the effects of window matching based sidereal filtering using different similarity measures when the template window size is set to different values. For case 1, the ED and CBD metrics perform well in the east and north components, but in the up component, lock-step metrics do not perform as well as the elastic metrics. For the east coordinate component, when the template window size is less than 40, the LCSS metric outperforms the ED metric, and when the template window size is greater than 40, the ED metric outperforms the LCSS metric. For the north coordinate component, the performance of the ED metric is always better than other metrics, and the performance of the CBD metric is also very good. For the up coordinate component, the elastic metrics are always better than the lock-step metrics, which may be due to the significant noise in the up component. For case 2, the LCSS metric performs better than other metrics, especially in the east and north coordinate components. ED performs well when the template window size is greater than 50 in the north and east coordinate components. The EDR metric performance is slightly better than the LCSS metric for the up coordinate component.

Table 5 RMS of coordinate time series in case 2 before and after processing by the proposed method based on different similarity metrics

	East		North		Up	
	RMS (mm)	Improvement (%)	RMS (mm)	Improvement (%)	RMS (mm)	Improvement (%)
Original	2.5782		3.4452		12.5354	
ED	1.2104	53.05	1.5714	54.39	5.8281	53.51
CBD	1.2379	51.99	1.5804	54.13	5.9219	52.76
FCBD	1.2143	52.90	1.5598	54.73	5.8047	53.69
DTW	1.2180	52.76	1.5597	54.73	5.9636	52.43
LCSS	**1.1729**	54.51	**1.5002**	56.45	5.6624	54.83
EDR	1.1826	54.13	1.5454	55.14	**5.6444**	54.97

Bold symbols represent the best measure in the experiment

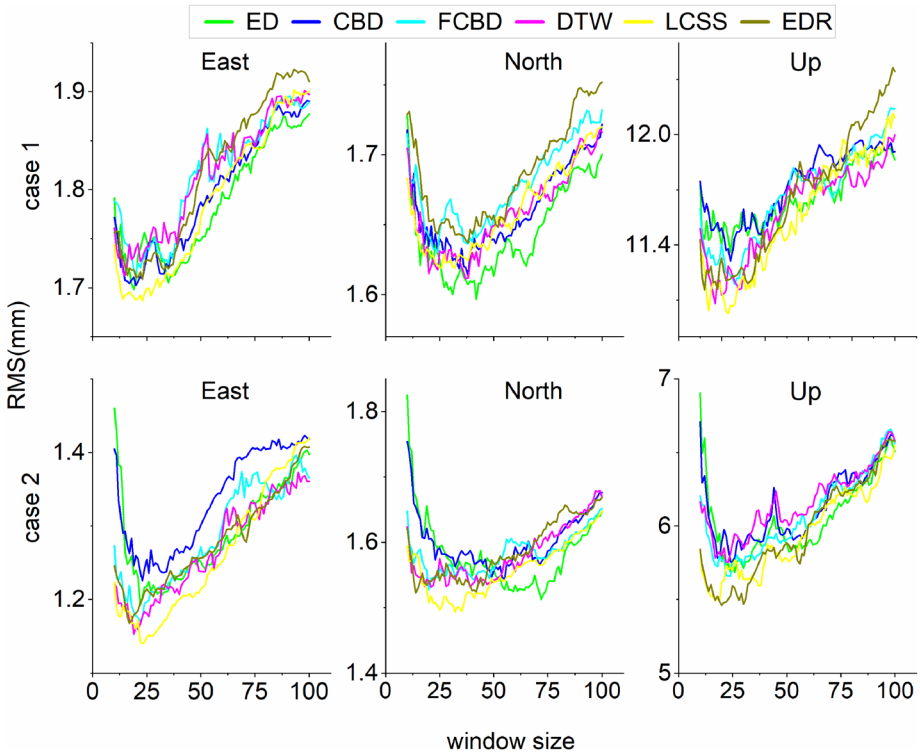

Fig. 13 Relationship between template window size and RMS of different similarity metrics. Top: statistical results of case 1; Bottom: statistical results of case 2

Through the above comparison, it can be concluded that the LCSS metric always performs well. Overall, elastic metrics are generally better than the lock-step metric, but under low noise conditions, ED and CBD perform well. In addition to the factors discussed above, there are also some factors that may affect the performance of the proposed algorithm, for example, the receiver's multipath suppression strategy at the hardware level.

Conclusions

We developed a method aiming at real-time sidereal filtering based on coordinate time series window matching between two consecutive days. The template window in window matching is formed by the current epoch and the previous epochs. The search window in window matching is roughly determined by the nominal sidereal day. The matching process is done through similarity measures. The multipath mitigation of the current epoch is carried out by an affine transformation based on the coordinate pairs of the matched window.

To validate the approach, we conducted two sets of short baseline experiments. In the first experiment, two geodetic receivers were used for two consecutive days of observations. In the second experiment, a geodetic receiver and a low-cost receiver were adopted for two consecutive days of observations. The two sets of observation data are processed by the proposed sidereal filtering method. The spectrum analysis of the processing results shows that the low-frequency component of multipath is effectively eliminated. The statistical analysis shows that the accuracy of the two groups of experiments is improved by about 26% and 53%, respectively.

Finally, we discuss the parameters of window matching: template window size and similarity measure. As the template window size increases, the RMS of the time series after filtering decreases first and then increases. The optimum template window size is around 30 for both cases. The LCSS metric always performs well in both experiments. The ED and CBD metrics perform well in the east and north components. Overall, the elastic measures perform better than the lock-step measures in the window matching.

Acknowledgements This research was funded by the National Key Research and Development Program (2016YFE0202300, 2018YFB0505400), the Zhejiang Lab's International Talent Fund for Young Professionals, and the Natural Science Fund of Hubei Province with Project No. 2018CFA007.

References

Agnew DC, Larson KM (2007) Finding the repeat times of the GPS constellation. GPS Solut 11(1):71–76

Atkins C, Ziebart M (2016) Effectiveness of observation-domain sidereal filtering for GPS precise point positioning. GPS Solut 20(1):111–122

Axelrad P, Larson K, Jones B (2005) Use of the correct satellite repeat period to characterize and reduce site-specific multipath errors. In: Proceedings of ION GNSS 2005, Institute of Navigation, Long Beach, CA, September 13–16, pp 2638–2648

Cai M, Chen W, Dong D, Song L, Wang M, Wang Z, Zhou F, Zheng Z, Yu C (2016) Reduction of kinematic short baseline multipath effects based on multipath hemispherical map. Sensors 16(10):1677

Chen L, Özsu MT, Oria V (2005) Robust and fast similarity search for moving object trajectories. In: Proceedings of the 2005 ACM SIGMOD international conference on Management of data, 2005, pp 491–502

Chen L, Simo A-L, Robert P, Wu L (2012) Mobile tracking in mixed line-of-sight/non-line-of-sight conditions: algorithm and theoretical lower bound. Wirel Pers Commun 65(4):753–771

Chen L, Piché R, Kuusniemi H, Chen R (2014) Adaptive mobile tracking in unknown non-line-of-sight conditions with application to digital TV networks EURASIP. J Adv Signal Process 1:22

Choi K, Bilich A, Larson KM, Axelrad P (2004) Modified sidereal filtering: implications for high-rate GPS positioning. Geophys Res Lett. https://doi.org/10.1029/2004gl021621

Fuhrmann T, Luo X, Knöpfler A, Mayer M (2015) Generating statistically robust multipath stacking maps using congruent cells. GPS Solut 19(1):83–92

Genrich JF, Bock Y (1992) Rapid resolution of crustal motion at short ranges with the global positioning system. J Geophys Res Solid Earth 97(B3):3261–3269

Giorgino Toni (2009) Computing and visualizing dynamic time warping alignments in R: the dtw package. J Stat Softw 31(7):1–24

Golay X, Kollias S, Stoll G, Meier D, Valavanis A, Boesiger P (1998) A new correlation-based fuzzy logic clustering algorithm for FMRI. Magn Reson Med 40(2):249–260

Groves PD, Jiang Z, Rudi M, Strode P (2013) A portfolio approach to NLOS and multipath mitigation in dense urban areas. In: Proceedings of ION GNSS 2013, Institute of Navigation, Nashville, TN, September 16–20, pp 3231–3247

Han S, Rizos C (1997) Multipath effects on GPS in mine environments. In: 10th international congress of the International Society for Mine Surveying Fremantle, Australia

Hofmann-Wellenhof B, Lichtenegger H, Collins J (2012) Global positioning system: theory and practice. Springer, Berlin

Hsu L-T (2017) GNSS multipath detection using a machine learning approach. In: 2017 IEEE 20th international conference on intelligent transportation systems (ITSC), Yokohama, Japan, August 16–19. IEEE

Jia Q, Wu R, Wang W, Lu D, Wang L (2018) Adaptive blind anti-jamming algorithm using acquisition information to reduce the carrier phase bias. GPS Solut 22(4):99

Jin S, Cardellach E, Xie F (2014) GNSS remote sensing. Springer, Dordrecht

Kollios G, Vlachos M, Gunopulos D (2002) Discovering similar multidimensional trajectories. In: Proceedings 18th international conference on data engineering, San Jose, CA, USA, February 26–March 1. IEEE, pp 673–684

Larson KM, Bilich A, Axelrad P (2007) Improving the precision of high-rate GPS. J Geophys Res Solid Earth. https://doi.org/10.1029/2006jb004367

Lau L (2012) Comparison of measurement and position domain multipath filtering techniques with the repeatable GPS orbits for static antennas. Surv Rev 44(324):9–16

Lau L, Cross P (2006) A new signal-to-noise-ratio based stochastic model for GNSS high-precision carrier phase data processing algorithms in the presence of multipath errors. In: Proceedings of ION GNSS 2006, Institute of Navigation, Fort Worth, TX, September 26–29, pp 276–285

Lau L, Cross P (2007) Development and testing of a new ray-tracing approach to GNSS carrier-phase multipath modeling. J Geodesy 81(11):713–732

Li D, Shao Z (2009) The new era for geo-information. Sci China Ser F Inf Sci 52(7):1233–1242

Li D, Yuan Y, Shao Z, Wang L (2010) From digital earth to smart earth. Chin Sci Bull 59(8):722–733

Mallat S (2008) A wavelet tour of signal processing: the sparse way, 3rd edn. Academic Press Inc, Orlando

Misra P, Enge P (2006) Global positioning system: signals, measurements, and performance, 2nd edn. Ganga-Jamuna Press, Massachusetts

Moore M, Watson C, King M, McClusky S, Tregoning P (2014) Empirical modelling of site-specific errors in continuous GPS data. J Geodesy 88(9):887–900

Ogaja C, Satirapod C (2007) Analysis of high-frequency multipath in 1-Hz GPS kinematic solutions. GPS Solut 11(4):269–280

Quan Y, Lau L, Roberts GW, Meng X, Zhang C (2018) Convolutional neural network based multipath detection method for static and kinematic GPS high precision positioning. Remote Sens 10(12):2052

Ragheb A, Clarke PJ, Edwards S (2007) GPS sidereal filtering: coordinate- and carrier-phase-level strategies. J Geodesy 81(5):325–335

Serrà J, Arcos JL (2014) An empirical evaluation of similarity measures for time series classification. Knowl-Based Syst 67:305–314. https://doi.org/10.1016/j.knosys.2014.04.035

Shao Z, Li D (2011) Image City sharing platform and its typical applications. Sci China Inf Sci 54(8):1738–1746

Shen N, Chen L, Liu J, Wang L, Tao T, Wu D, Chen R (2019) A review of global navigation satellite system (GNSS)-based dynamic monitoring technologies for structural health monitoring. Remote Sens. https://doi.org/10.3390/rs11091001

Strode PR, Groves PD (2016) GNSS multipath detection using three-frequency signal-to-noise measurements. GPS Solut 20(3):399–412

Takasu T (2011) RTKLIB: an open source program package for GNSS positioning. Technical Report, 2013. Software and Documentation

Townsend B, Fenton P, Van Dierendonck K, Van Nee R (1995) L1 carrier phase multipath error reduction using MEDLL technology. In: Proceedings of ION GPS 1995, Institute of Navigation, Palm Springs, CA, September 12–15, pp 1539–1544

Wang X, Mueen A, Ding H, Trajcevski G, Scheuermann P, Keogh E (2013) Experimental comparison of representation methods and distance measures for time series data. Data Min Knowl Discov 26(2):275–309

Wang M, Wang J, Dong D, Li H, Han L, Chen W (2018) Comparison of three methods for estimating GPS multipath repeat time. Remote Sens 10(2):6

Ye S, Chen D, Liu Y, Jiang P, Tang W, Xia P (2015) Carrier phase multipath mitigation for BeiDou navigation satellite system. GPS Solut 19(4):545–557

Zhang Z, Li B, Gao Y, Shen Y (2019) Real-time carrier phase multipath detection based on dual-frequency C/N0 data. GPS Solut 23(1):7

Nan Shen is currently a Ph.D. student at State Key Laboratory of Information Engineering in Surveying, Mapping and Remote Sensing at Wuhan University. His research interests focus on precise GNSS data processing, software-defined receiver.

Liang Chen is a professor of State Key Laboratory of Surveying, Mapping and Remote Sensing Information Engineering, Wuhan University. His research interests include navigation of new signal theory and method, ubiquitous smartphone positioning, and indoor and outdoor seamless positioning and navigation.

Lei Wang is currently an associate research fellow at State Key Laboratory of Information Engineering in Surveying, Mapping and Remote Sensing at Wuhan University. His research interests include GNSS precise positioning and LEO navigation augmentation system.

Xiangchen Lu is currently a master student at State Key Laboratory of Information Engineering in Surveying, Mapping and Remote Sensing at Wuhan University. His main research direction is software-defined receivers.

Tingye Tao is an associate professor at the College Civil Engineering at the Hefei University of Technology. His research interests include GNSS precise positioning and deformation monitoring.

Jun Yan is an associate professor at the College of Telecommunications and Information Engineering, Nanjing University of Posts and Telecommunications. His research interests include wireless positioning technology based on machine learning and intelligent signal processing technology.

Ruizhi Chen is a professor of State Key Laboratory of Surveying, Mapping and Remote Sensing Information Engineering, Wuhan University, and director of the laboratory. His main research interests include smartphone ubiquitous positioning and satellite navigation and positioning.